Microstructure in A356/AA6xxx after bimetallic casting with flux coating

Microstructure in A356/AA6xxx after bimetallic casting with flux coating

Aina Opsal Bakke[1], Lars Arnberg[1] and Yanjun Li[1]

[1]Department of Materials Science and Engineering, Norwegian University of Science and Technology, Trondheim, Norway

Corresponding author: aina.o.bakke@ntnu.no

Abstract. This work focuses on bimetallic casting between A356 alloy melt and profiles of AA6xxx wrought aluminum alloys through a gravity casting process, with the aim to improve the component's mechanical properties. However, combining two aluminum alloys is difficult due to the stable aluminum oxide present on the surface of the aluminum inserts and the advancing liquid melt front. The oxide layer strongly reduces the wettability between aluminum melt and solid metal. It will also prevent diffusion and formation of a metallurgical bond. In order to obtain sound metallic bonding between the two alloys, different surface treatments, including flux coating and chemical treatments of the profiles have been tested. The influences of preheating temperature and melt flow modes on the quality of the bimetallic casting have been addressed. Based on a detailed microstructure characterization of the bonding layer in the casting, by using Optical Microscopy (OM), Scanning Electron Microscopy (SEM) and Energy Dispersive X-ray Spectroscopy (EDS), the solidification structure development at the interface has been discussed. Results showed that when flux coating was applied, magnesium diffused to the insert surface and prevented formation of a metallurgical bond. Without flux coating, a metallurgical bond was achieved due to slight melting of the insert surface.

1. Introduction

Joining of two aluminum alloys have gained interest, especially in the automotive industry, as aluminum with its high strength-to-weight ratio [1] can replace heavier materials to achieve weight reduction, thus also reduce emission from the vehicles. Such a multi-material is also beneficial, as it is able to meet specific requirements that one material alone often cannot.

Bimetallic casting, also known as compound casting, is a process in which two materials, one solid and one liquid are joined together. The solid material will be placed in the mold prior to casting, where the liquid material is cast around, creating a diffusion zone between the two materials which leads to a metallurgical bond [2]. Although several other processes have been used to join aluminum, such as friction stir welding [3], explosive welding [4], gas metal arc welding [5] and direct chill casting [6], bimetallic casting has in general higher process efficiency and less geometric limitations.

The difficulty in joining aluminum alloys is mainly due to the surface oxide layer. Aluminum oxides form spontaneously and are thermodynamically stable [7], while their melting points are significantly higher than typical process temperatures [8]. Due to this stability, the oxides reduce wettability of the aluminum surface, which hinders formation of a metallurgical bond [9]. To remove surface oxides, aluminum is often pickled or etched and then coated with a material to prevent reoxidation. Use of zinc as coating has showed good potential, as it melts at a low temperature and thus allows for bonding with

an aluminum surface free of oxides [9] [10] [11]. Coating with Ni and Cu has also shown formation of a metallurgical bond between a cast and a wrought aluminum alloy [12].

In this research, a wrought and a cast aluminum alloy has been joined through a bimetallic casting process. Various flux coatings have been used to remove oxides from the aluminum surface and thus enhance wettability. The flux coatings are typically used for brazing, and therefore the parameters in the bimetallic casting will resemble those of a brazing process. Microstructure in the interface has been investigated and discussed.

2. Experimental procedure

6060 aluminum bolts with a diameter of 10mm, were cut to lengths of 10cm. Prior to casting, the bolts were ground with 1200grit sandpaper and cleaned with ethanol, before being immersed into a bath of 10% HCl for 30sec followed by further cleaning in distilled water and then ethanol. This was to remove some of the surface oxides. A third of the bolts were then coated with a liquid flux consisting of $K_{1-3}AlF_{4-6}$, $KZnF_3$, Li_3AlF_6 and metallic silicon particles [13]. Another third was coated with a mixture of $K_{1-3}AlF_{3-6}$ and $CsAlF_4$ [14]. The Cs containing flux was mixed with distilled water to a concentration of approximately 51%. The mixture was then painted on the bolts. The remaining third was left without surface treatment.

The treated 6060 aluminum bolt was then inserted into a graphite mold. A sketch of the mold is shown in Figure 1. Both the mold and the insert were heated to 600°C prior to casting. An A356 alloy was melted in an induction furnace to 730°C. Composition of both aluminum alloys are given in Table 1. Casting was performed at a pouring temperature of 720°C. After pouring, the mold remained in the furnace at 600°C for five minutes before being removed and air-cooled.

Table 1 Chemical composition of aluminum alloys 6060 and A356

Alloy	Composition [wt.%]									
	Mg	Si	Fe	Zn	Cu	Mn	Ti	Cr	Others	Al
6060 [13]	0.45-0.6	0.3-0.6	0.1-0.3	0.15	0.1	0.1	0.1	0.05	0.05-0.15	Bal.
	Si	Mg	Ti	Fe	Sr	Ga	Zn	Others	Al	
A356	7.0	0.41	0.11	0.082	0.013	0.0089	0.0042	0.0029	Bal.	

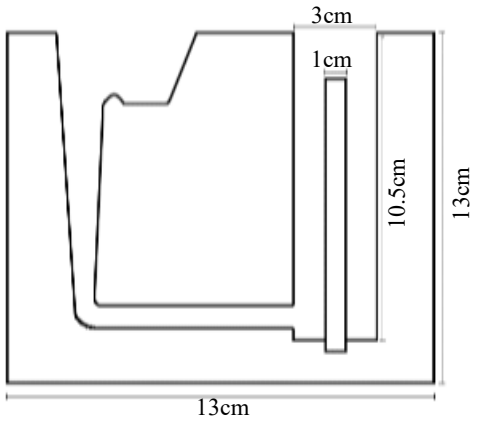

Figure 1 Sketch and dimensions of the graphite mold

2.1. Materials characterization

Samples of 1cm thickness were cut perpendicular to the bolt from each casting. These were ground to 4000 grits using a Struers LaboPol-21, then polished with diamond suspension of 3µm and 1µm on a Struers Tegramin-20. A Leica MEF4M optical microscope was used to examine the interface and the bonding properties between the aluminum alloys. To characterize and detect the elements in the

interface, a Zeiss Supra 55VP Field Emission Scanning Electron Microscope (FESEM) with Energy Dispersive X-ray Spectroscopy (EDS) was used. A working distance of 10mm and an acceleration voltage of 15kV were applied in the FESEM observation.

3. Results

3.1. Effect of flux coating

The samples from the two different flux coatings will in the results be mentioned as SF and SN, where SF is the sample coated with the liquid flux, while SN is the sample coated with Cs flux. Figure 2 shows optical micrographs of the 6060/A356 interface in the two flux coated samples.

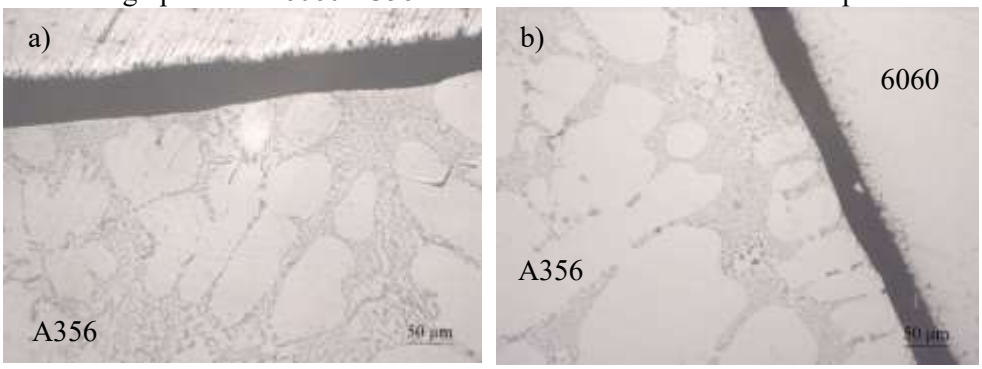

Figure 2 Optical micrographs of the 6060/A356 interface in the flux-coated castings a) With liquid flux (SF) and b) With Cs flux (SN)

As seen in Figure 2, there is a significant gap between the 6060 insert and the cast A356 for both flux-coated castings. This gap was seen throughout the interfaces and shows that no metallic bonding was achieved for either casting. For casting SF the gap width average was measured to approximately 40µm, while it was slightly thinner for SN measuring to approximately 30µm. Also visible in the micrographs, are the relatively large dendrites in the cast alloy. The mold remaining at 600°C for five minutes significantly decreases the cooling rate and allows the dendrites to grow. Average secondary dendrite arm spacing (SDAS) was measured to approximately 65µm for SF and 73µm for SN.

To further examine the interface, an EDS analysis was performed at areas close to the gap on the 6060 insert. The areas analyzed are shown in Figure 3, where backscattered electron (BSE) imaging is used to see the different atom contrasts. By observing the micrographs, there appears to be some flux remaining on the 6060 insert in casting SF (Figure 3a). However, for casting SN (Figure 3b), there is definitely something remaining on the insert, as a porous material can be observed in the interface. This was observed across the whole interface from the edge of the 6060 insert to the cast A356, indicating that indeed something has remained in the interface.

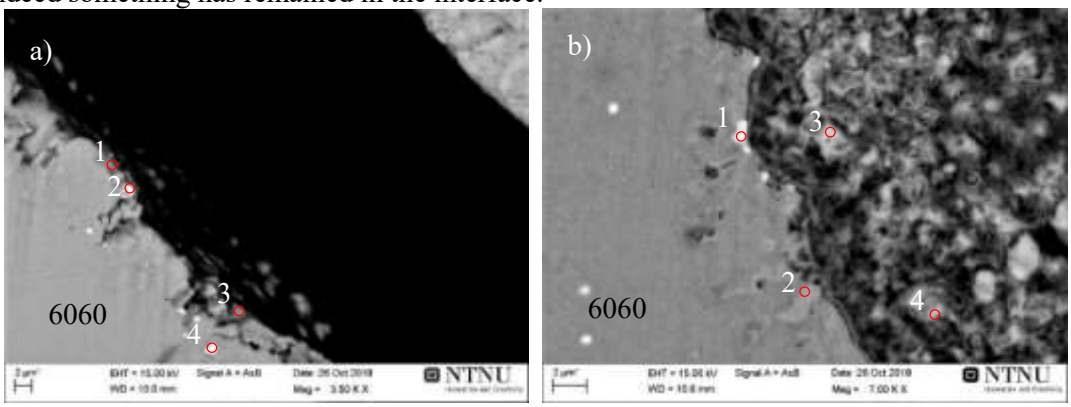

Figure 3 Micrographs of the 6060 surface in casting a) SF and b) SN

Table 2 Compositions detected through EDS analysis at the surface of the 6060 insert in castings SF and SN

Area	Composition [at%]							
	C	O	F	Mg	Al	Si	K	Fe
A-1	41.55	19.70	4.38	1.04	31.31	1.61	0.40	-
A-2	39.33	24.22	-	-	31.85	2.88	-	1.73
A-3	53.73	29.08	4.89	1.26	10.02	0.43	0.60	-
A-4	-	-	28.59	12.00	49.27	-	10.14	-
B-1	-	16.83	17.52	6.47	44.71	3.40	5.19	5.88
B-2	-	5.36	27.38	9.56	49.23	-	8.47	-
B-3	13.97	22.14	33.01	-	13.54	-	17.34	-
B-4	19.92	24.24	28.65	-	13.03	-	14.17	-

The EDS results in Table 2 show that potassium and fluorine are detected in nearly all analyzed areas, which are two of the main elements in the two flux coatings. This implies that the flux coating still remains on the insert after casting. Interestingly, high concentrations of magnesium have also been detected at the insert surface. 6060 has a magnesium content of 0.4-0.6wt%, which is below all the concentrations detected in the EDS analysis. In combination with the potassium and fluorine concentrations found, this could suggest diffusion of magnesium to the surface, and formation of K-F-Mg of F-Mg phases. Especially Area A-4 is believed to be a ternary K-F-Mg phase.

In Area A-2 and B-1, iron is detected. Considering that both these areas are white particles, it is likely that these particles are similar. Although fluorine, magnesium and potassium are also detected in Area B-1, it is suggested that these white particles are Al-Fe-Si ternary particles as they are observed further in the insert as well. The high concentration of oxygen shows that there might be oxides at the surface. Comparing the EDS analysis of the two different flux coatings, it is evident that a higher concentration of flux coating has remained in the interface of casting SN.

3.2. Bimetallic casting without flux coating

When analyzing the sample without flux coating, it was possible to see that the outer part of the insert had melted. This was also observed in the optical microscope, as the insert no longer displayed a circular form. In higher magnification, it was possible to see that due to the melting, a metallurgical bond had formed between the insert and the cast alloy. Figure 4 shows an optical micrograph of the 6060/A356 interface, where the transition from cast to wrought alloy can be distinguished by the characteristic eutectic silicon in A356.

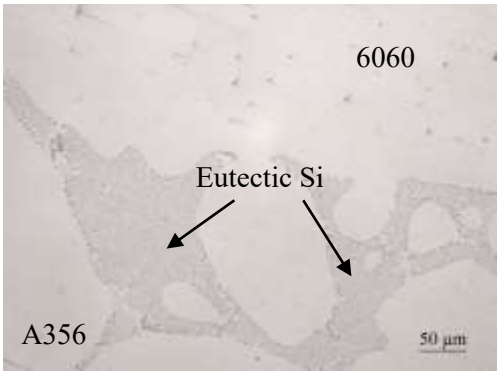

Figure 4 Optical micrograph of the 6060/A356 interface in the non-coated sample. No gap can be observed between the two alloys

Although a metallurgical bond formed in the non-coated casting, cracks were still observed in certain areas. As seen in Figure 5a, the crack propagates through the cast A356, following a path through the interdendritic eutectic silicon. Figure 5b shows that the crack continues through the eutectic silicon at the 6060/A356 interface, as silicon can be observed on both sides. This shows that

the crack has formed mainly in the A356 alloy side upon solidification, likely due to built-up stress as aluminum shrinks upon cooling and solidification.

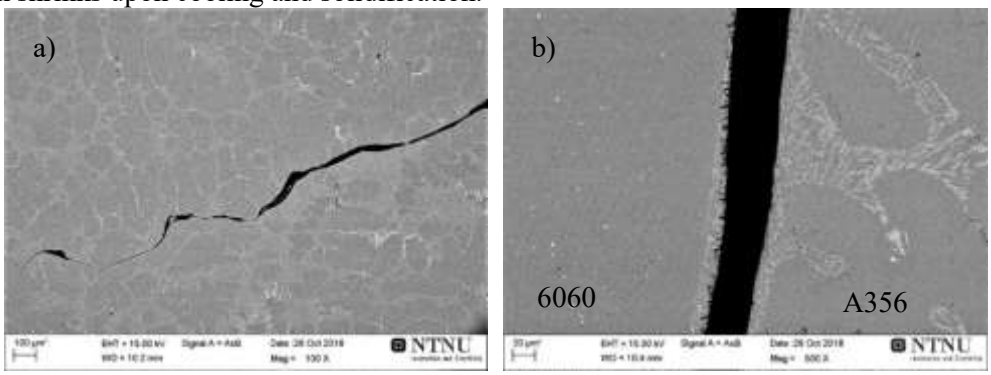

Figure 5 Micrographs of the crack observed in the non-coated casting. Crack propagating through the eutectic Si a) In the cast A356. b) Adjacent to the 6060/A365 interface

4. Discussion

4.1. Formation of a metallurgical bond

According to the manufacturer's specifications, the 6060 aluminum inserts have a melting range of 555-660°C [13]. This means that a preheating temperature of 600°C is well above the solidus temperature of the 6060 alloy. Upon casting, the insert is further heated due to the pouring temperature of 720°C. The outer layer will then remelt, causing a liquid-liquid interface and the formation of a metallurgical bond. It has been suggested that the bond forms due to interdiffusion of the alloying elements, and that through a liquid-liquid reaction no treatment to remove the oxide layers was necessary [6] [14]. The interface between the two alloys can be recognized from the eutectic silicon structure observed in the A356 alloy. In the non-coated casting, the only defect observed was the crack propagating through the eutectic silicon. As aluminum cools and solidifies, it shrinks and thus creates stresses at the interface that in this case has resulted in a crack.

4.2. Flux coating reactions

According to the product description of the fluxes, the liquid flux has a melting range of 564-572°C [15], while it is 558-566°C for the Cs flux [16]. This implies that under the conditions used in the experiment, the flux should be molten and ready to react with the surface oxides. As mentioned for the non-coated casting, the preheating temperature was sufficient to melt the outer layer of the insert. However, for both flux coatings, no change in the insert shape was observed, suggesting that no melting had occurred. It has previously been reported that K_xAlF_y fluxes are highly reactive with magnesium. Therefore, solute magnesium atoms in the 6060 insert will diffuse towards the flux layer and form compounds such as MgF_2 and $KMgF_3$, which due to their high melting points will reduce the flux efficiency [17]. The EDS analysis in Table 2 shows magnesium at the insert surface exceeding that of the 6060 alloy composition provided in Table 1. As the mold and insert are kept in the furnace until the preheating temperature is reached, it allows for solid-state diffusion of magnesium in the insert. Since such magnesium compounds were found, they have probably decreased the flux' efficiency and wettability so that upon casting no bonding will occur.

Comparing the two fluxes, the Cs flux shows in general a slightly thinner gap. However, this could be due to the flux drying upon heating allowing it to shrink slightly, while the liquid flux remains as a paste. Based on the element detection on the insert surface and in the interface, and that the gap had approximately similar width throughout the interface, it is believed that the flux coating remained on the interface after casting for both fluxes. Overall, lower concentrations of magnesium is detected on the insert surface using the liquid flux. This could be due to the lower concentration of K_xAlF_y in the liquid flux compared to the Cs flux.

5. Conclusions

Metallurgical bonding between 6060/A356 aluminum could be achieved without flux coating. The preheating temperature of the insert allowed for a slight melting of the insert surface, promoting formation of a metallic bond.

Using flux coating containing K_xAlF_y prevented a metallurgical bond due to diffusion of magnesium to the insert surface and formation of magnesium compounds with high melting points. It also prevented remelting of the 6060 insert surface.

6. Acknowledgements

The authors would like to thank the Research Council of Norway for financial support through the IPN project “AluLean” (90141902).

References

[1] Miller, W., Zhuang, L., Bottema, J., Wittebrood, A., De Smet, P., Haszler, A., & Vieregge, A. (2000). *Materials Science and Engineering: A*, **280**(1), 37-49.
[2] Tayal, R. K., Singh, V., Kumar, S., & Garg, R. (2012). *Proceedings of the National Conference on Trends and Advances in Mechanical Engineering,* 501-510.
[3] Prime, M. B., Gnäupel-Herold, T., Baumann, J. A., Lederich, R. J., Bowden, D. M., & Sebring, R. J. (2006). *Acta Materialia*, **54**(15), 4013-4021.
[4] Findik, F. (2011). *Materials & Design*, **32**(3), 1081-1093.
[5] Praveen, P., & Yarlagadda, P. K. (2005). *Journal of Materials Processing Technology,* **164-165**, 1106-1112.
[6] Fu, Y., Jie, J., Wu, L., Park, J., Sun, J., Kim, J., & Li, T. (2013). *Materials Science and Engineering: A*, **561**, 239-244.
[7] Papis, K. J., Loeffler, J. F., & Uggowitzer, P. J. (2009). *Science in China, Series E: Technological Sciences*, **52**(1), 46-51.
[8] Aylward, G., & Findlay, T. (2002). *SI Chemical Data* (5th ed.). Milton: John Wiley & Sons Australia.
[9] Papis, K. J., Hallstedt, B., Löffler, J. F., & Uggowitzer, P. J. (2008). *Acta Materialia*, **56**(13), 3036-3043.
[10] Liu, T., Wang, Q.-d., Liu, P., Sun, J.-w., Yin, X.-l., & Wang, Q.-g. (2015). *Transactions of Nonferrous Metals Society of China*, **25**, 1064-1072.
[11] Koerner, C., Schwankl, M., & Himmler, D. (2014). *Journal of Materials Processing Technology*, 1094-1101.
[12] Feng, J., Ye, B., Zuo, L., Wang, Q., Wang, Q., Jiang, H., & Ding, W. (2017). *Metallurgical and Materials Transactions A*, **48A**, 4632-4644.
[13] Solvay. (2017, December 22). Safety Data Sheet - Nocolok® Sil Flux - Fine Grade. Retrieved from https://www.solvay.us/en/binaries/P02-19419-USA_CN_EN-237549.pdf
[14] Solvay. (2017, March 3). Safety Data Sheet - NOCOLOK®Cs FLUX (TM) BW. Retrieved from https://www.solvay.us/en/binaries/P36966-USA_CN_EN3-238040.pdf
[15] Smith Stål. Smith Stål - Storage catalogue. Retrieved from https://www.smithstal.no/SmithStaal/Produkter/lagerkatalog-smithstal.no.pdf
[16] Sun, J., Song, X., Wang, T., Yu, Y., Sun, M., Cao, Z., & Li, T. (2012). *Materials Letters*, **67**(1), 21-23.
[17] Takemoto, T., Matsunawa, A., & Shibutani, T. (1997). *Welding International*, **11**(11), 845-851.